ARTICLE

OBC
www.rsc.org/obc

Bisubstrate inhibitors for the enzyme catechol-*O*-methyltransferase (COMT): influence of inhibitor preorganisation and linker length between the two substrate moieties on binding affinity

Christian Lerner,[a] Birgit Masjost,[a] Armin Ruf,[b] Volker Gramlich,[c] Roland Jakob-Roetne,[b] Gerhard Zürcher,[b] Edilio Borroni[b] and François Diederich*[a]

[a] *Laboratorium für Organische Chemie, ETH-Hönggerberg, HCI, CH-8093 Zürich, Switzerland*

[b] *Pharma Division, Präklinische Forschung, F. Hoffmann-La Roche AG, CH-4070 Basel, Switzerland*

[c] *Laboratorium für Kristallographie, ETH-Zentrum, Sonneggstrasse 5, CH-8092 Zürich, Switzerland*

Received 5th September 2002, Accepted 7th October 2002
First published as an Advance Article on the web 26th November 2002

Inhibition of the enzyme catechol-*O*-methyltransferase (COMT) is an important approach in the treatment of Parkinson's disease. A series of new potent bisubstrate inhibitors for COMT, resulting from X-ray structure-based design and featuring adenosine and catechol moieties have been synthesised. Biological results show a large dependence of binding affinity on inhibitor preorganisation and the length of the linker between nucleoside and catechol moieties. The most potent bisubstrate inhibitor for COMT has an IC_{50} value of 9 nM. It exhibits competitive kinetics for the SAM and mixed inhibition kinetics for the catechol binding site. Its bisubstrate binding mode was confirmed by X-ray structure analysis of the ternary complex formed by the inhibitor, COMT and a Mg^{2+} ion.

Introduction

Inhibitors, where a substrate analogue and a cofactor analogue are covalently linked to form a bisubstrate inhibitor, may offer opportunities for specificity and activity in blocking therapeutically important enzymes that are not available to simple substrate analogues.[1] In principle, any enzyme that catalyses chemical transformations between two or more bound substrates or a substrate and a cofactor is a plausible candidate for the design of multisubstrate inhibitors. Recent examples of enzymes targeted with bisubstrate inhibitors are the insulin receptor tyrosine kinase,[2] farnesyltransferase,[3,4] serotonin-*N*-acetyltransferase[5] and acetyl-CoA-carboxylase.[6] Other important targets are methyltransferases that depend on *S*-adenosylmethionine (SAM).

The enzyme catechol-*O*-methyltransferase (COMT) catalyses the methyl group transfer from the cofactor SAM to the phenolic hydroxy group of catechol-type substrates, such as L-dopa and dopamine, in the presence of magnesium ions. The inhibition of COMT is of significant interest in the treatment of Parkinson's disease.[7] The symptoms of Parkinson's disease are a consequence of a low level of the neurotransmitter dopamine in the brain. Current therapies increase the dopamine level by oral administration of L-dopa, which is decarboxylated to dopamine by the enzyme aromatic amino acid decarboxylase (AAD). L-Dopa is able to cross the blood brain barrier, whereas dopamine is not. To avoid decarboxylation in the periphery, L-dopa is given in combination with an inhibitor for the decarboxylase which cannot cross the blood brain barrier. When AAD is inhibited, deactivation by COMT becomes the major metabolic pathway for L-dopa in the periphery. Inhibition of COMT increases the elimination half-time of L-dopa, ensuring that a larger quantity of orally administered L-dopa reaches its target in the brain.[7]

Nitro-substituted catechols were found to be potent COMT inhibitors, and two derivatives, tolcapone (Tasmar®)[8] and entecapone (Comptan®)[9] have been introduced into the marketplace. Using rational design based on the X-ray crystal structure of COMT,[10,11] we developed the first effective bisubstrate inhibitor **1** for COMT (IC_{50} = 2 μM; IC_{50} = concentration of inhibitor at which 50% V_{max} is observed), featuring both nucleoside and catechol moieties for occupancy of the SAM and substrate binding sites, respectively.[11,12] Here, we report the synthesis and biological evaluation of a new series of bisubstrate inhibitors **2**–**6** reaching binding activities in the single-digit nanomolar range (compound **2**).[13] We show that affinity for COMT strongly depends on the size and shape of the linker between the nucleoside and catechol moieties. The bisubstrate inhibition mode of **2** was confirmed by kinetic analysis and the principles of molecular recognition governing complex formation elucidated by X-ray crystal structure analysis of the ternary complex formed between **2**, COMT and a Mg^{2+} ion.

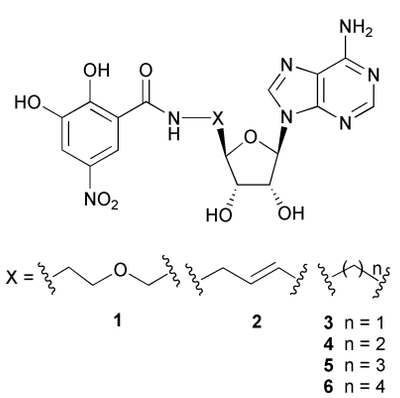

Results and discussion

Inhibitor design

For a cytosine analogue of **1**, ^{1}H NMR conformational analysis in D_2O had revealed a strong nuclear Overhauser effect (NOE) between the catechol protons and H–C(5) of the nucleobase, indicating hydrophobic collapse of the unbound inhibitor.[14] In the collapsed conformation, the catechol moiety does not adopt

DOI: 10.1039/b208690p

the right orientation to bind to the active site of COMT and, therefore, upon binding significant reorganisational energy would be required. Additionally, the solvation of a collapsed conformation of the inhibitor is particularly favourable, which further reduces the measurable binding free energy. Therefore, we were interested in increasing its degree of preorganisation [15] prior to complexation. To prevent hydrophobic collapse in the unbound state, the new inhibitors **2**–**6** with shorter and conformationally less flexible linkers between nucleoside and catechol moieties were designed using the molecular modeling program MOLOC [16] with the MAB force field. For the exploration of their geometric and electronic complementarity to the enzyme active site, the proposed inhibitors were docked manually into this site by overlaying their catechol and nucleoside parts on 3,5-dinitrocatechol and SAM of the X-ray crystal structure of COMT,[10,11] and subsequently energy-minimized, while the coordinates of COMT and the Mg^{2+} ion were constrained. Within the series of inhibitors **3**–**6** with various linker sizes, the three-carbon bridge in **5** was predicted to provide the best geometric fit for bisubstrate binding. A particularly favourable binding mode was predicted for **2** with a spacer rigidified by introduction of a *trans* double bond.

Synthesis

The activated ester **7** [11] reacted selectively with the primary amino group of 5′-amino-2′,3′-*O*-isopropylidene-5′-deoxyadenosine **8** [17] to give inhibitor **3** (Scheme 1). Generally, attempts

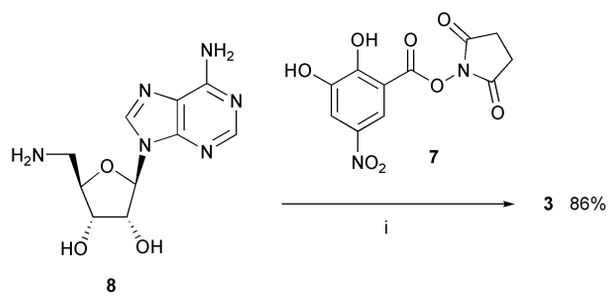

Scheme 1 Synthesis of inhibitor **3**. *Reagents and conditions*: (i) Et_3N, DMF, 20 °C.

to obtain pure inhibitors by recrystallisation were not reliable and gave poor yields. Due to the highly polar nature of the nitrocatechol derivatives, purification by column chromatography on SiO_2 was also not possible. Therefore, reverse phase chromatography on SiO_2 100 C_{18} became the method of choice for purification of the target compounds, using MeCN/1% aq. HCOOH mixtures as eluent.

For the synthesis of inhibitor **4**, 2′,3′-*O*-isopropylideneadenosine **9** [18] was transformed in high yield (89%) into nitrile **10** [19] using the Mitsunobu–Wilk procedure,[20] with acetone cyanohydrin as the cyanide ion source (Scheme 2). This method

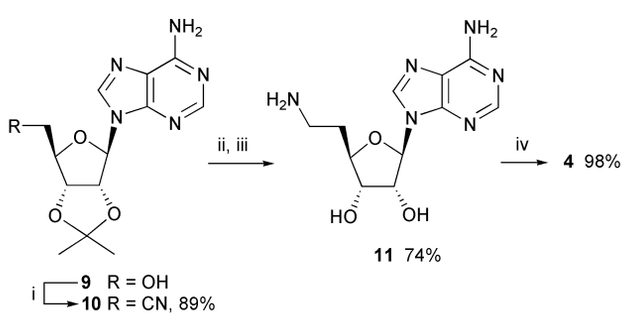

Scheme 2 Synthesis of inhibitor **4**. *Reagents and conditions*: (i) acetone cyanohydrin, PPh_3, DEAD, THF, 0 °C ⟶ 20 °C; (ii) PtO_2, AcOH, H_2, 20 °C; (iii) TFA–H_2O (5:2), 20 °C, then Dowex® 50 Wx4 (NH_4^+); (iv) Et_3N, DMF, 20 °C.

gave much better yields than the previously reported [19] reaction of 2′,3′-*O*-isopropylidene-5′-*O*-tosyladenosine with potassium cyanide in the presence of [18]crown-6. Reduction of nitrile **10** was accomplished by hydrogenation using platinum oxide in acetic acid; attempts using other catalysts or solvents failed. Subsequent deprotection afforded amine **11**,[21] purified by ion exchange chromatography, which reacted with the activated ester **7** to give inhibitor **4** in excellent yield (98%) after purification by reversed-phase chromatography.

In the synthesis of inhibitors **2** and **5**, we initially used published procedures [22,23] to synthesize the unsaturated ester **12** starting from **9**. However, oxidation to the aldehyde under the conditions of Pfitzner and Moffat,[24] followed by a Wittig reaction, gave only low yields. One-pot 5′-oxidation with *ortho*-iodoxybenzoic acid (IBX) followed by olefination with $Ph_3P{=}CHCO_2Et$ [25] was more effective (Scheme 3). Reduction with

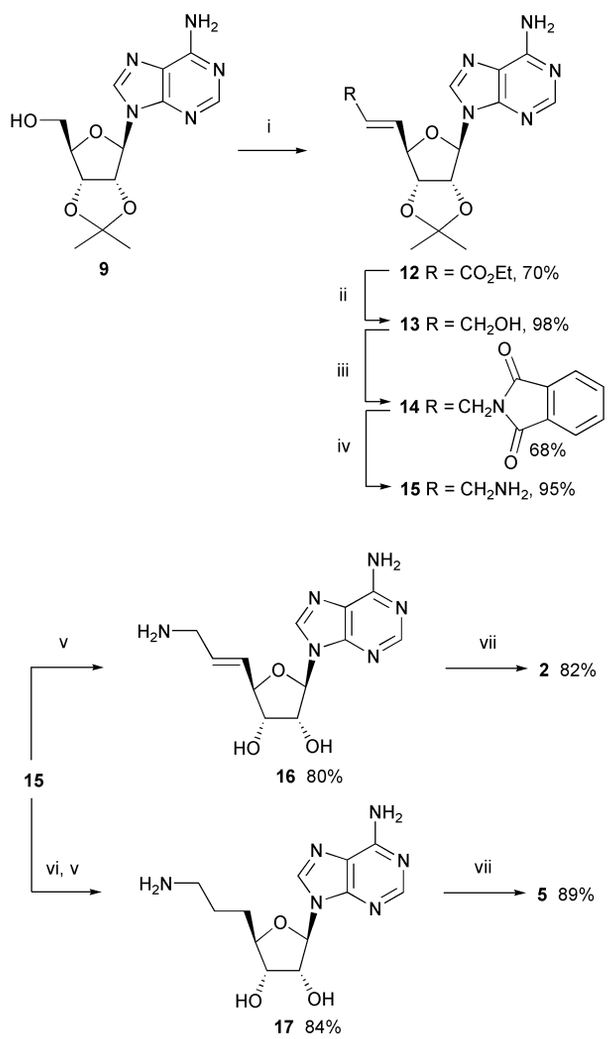

Scheme 3 Synthesis of inhibitors **2** and **5**. *Reagents and conditions*: (i) *o*-iodoxybenzoic acid (IBX), $Ph_3P{=}CHCO_2Et$, Me_2SO, 20 °C; (ii) DIBAL-H, hexane, CH_2Cl_2, −78 °C; (iii) phthalimide, DEAD, PPh_3, THF, 20 °C; (iv) $MeNH_2$, EtOH, 20 °C; (v) TFA–H_2O (5:2), 20 °C, then Dowex® 50 Wx4 (NH_4^+); (vi) H_2, Pd/C, EtOH, 20 °C; (vii) Et_3N, DMF, 20 °C.

DIBAL-H gave the allylic alcohol **13** in very good yield (98%), which was transformed into phthalimide **14** by a Mitsunobu reaction. The X-ray crystal structure of **14** [13] showed a large spatial separation of the nucleobase and phthalimide moieties, indicating that an alkene spacer would effectively prevent a hydrophobic collapse of the free bisubstrate inhibitor **2** (Fig. 1).

Cleavage of phthalimide **14** with methylamine [26] gave amine **15** in better yield than the reaction using toxic hydrazine.

Table 1 IC_{50} values (uncertainties ± 5 %), determined by radiochemical assay with preincubation,[11,27] for the bisubstrate inhibitors **1**–**6** of COMT

Compound	IC_{50}/μM
1	2
2	0.009
3	90
4	0.06
5	0.2
6	5

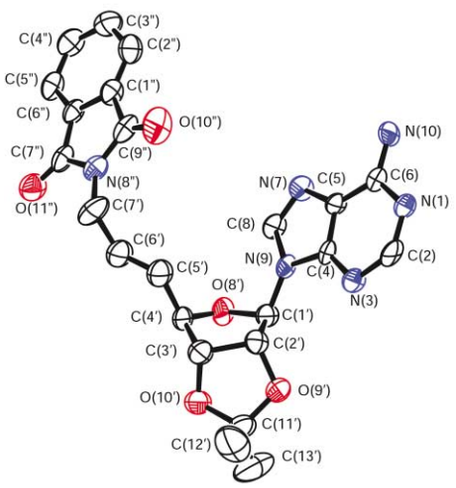

Fig. 1 X-Ray crystal structure of **14**. Arbitrary numbering. Thermal ellipsoids are shown at the 50% probability level.

Deprotection and purification of **15** by ion exchange chromatography led to **16**, which reacted with **7** to provide bisubstrate inhibitor **2** with a rigidified olefinic linker.

Catalytic hydrogenation of allylic amine **15**, followed by deprotection with TFA–H_2O (5:2) and removal of TFA by ion exchange chromatography gave **17** which was coupled to **7** to give the target compound **5**.

In the preparation of **6**, catalytic hydrogenation of allylic alcohol **13** followed by Mitsunobu–Wilk cyanation[20] gave nitrile **18** which was reduced and deprotected (Scheme 4).

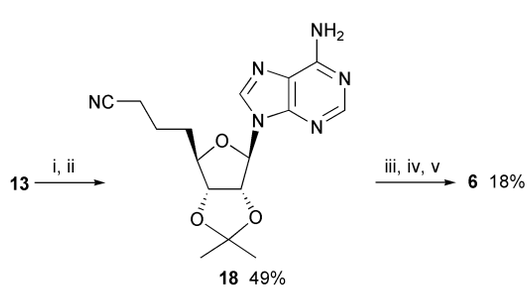

Scheme 4 Synthesis of inhibitor **6**. *Reagents and conditions*: (i) H_2, Pd/C, EtOH, 20 °C; (ii) acetone cyanohydrin, PPh_3, DEAD, THF, 0 °C ⟶ 20 °C; (iii) PtO_2, AcOH, H_2, 20 °C; (iv) TFA–H_2O (5:2), 20 °C; (v) Et_3N, DMF, 20 °C.

Purification of the resulting free primary amine proved problematic, therefore the crude product was eventually coupled to **7** to provide **6**.

Biological results

The IC_{50} values were determined in a radiochemical assay as previously reported[11,27] and are listed in Table 1. In the assay, the enzyme is preincubated with varying concentrations of inhibitor in a buffered aqueous solution containing Mg^{2+} ions for 15 min at 37 °C giving the system time to establish an equilibrium. The reaction is started by adding the cofactor SAM which carries a tritylated methyl group and the substrate benzene-1,2-diol. After incubation for 15 min at 37 °C, the reaction is quenched by addition of acetic acid and an organic scintillation fluid is added. The product (^{3}H)-2-methoxyphenol is extracted into the organic phase, whereas (^{3}H)-SAM remains in the aqueous phase. The product concentration is measured by counting the decays per min (dpm) in the organic phase. The dpm are proportional to the concentration of the reaction product, which is a measure for the enzymatic activity.

As expected, the linker of **3** was too short to provide effective bisubstrate binding (IC_{50} = 90 μM). Somewhat unexpectedly, compound **4** with a two-carbon linker showed a lower IC_{50} value (60 nM) than inhibitor **5** with a three-carbon bridge (200 nM). The four-carbon linker used in **6** (IC_{50} = 5 μM), similar to the four-atom linker in **1** (IC_{50} = 2 μM), seems to be too long. Clearly, the spacers in **4** and **5** have the best length to allow docking in both the SAM and the catechol binding sites. Further rigidification of the spacer by introduction of a *trans* double bond had a tremendous effect on binding affinity. Compound **2**, with an IC_{50} value of 9 nM, is the most potent bisubstrate inhibitor for COMT to date.

To investigate the mechanism of enzyme inhibition by **2**, kinetic studies were performed.[11] Initial velocities were determined without preincubation. K_i values were calculated by globally fitting the data to eqn. (1) or (2), corresponding to linear competitive or mixed inhibition, respectively. In these equations, K_{ic} and K_{iu} are competitive and uncompetitive inhibition constants, respectively.

$$v = V[S]/(K_m(1 + [I]/K_{ic}) + [S]) \quad (1)$$

$$v = V[S]/(K_m(1 + [I]/K_{ic}) + [S](1 + [I]/K_{iu})) \quad (2)$$

Inhibitor **2** showed a competitive inhibition mechanism with regard to the SAM binding site (Fig. 2), and had a K_{ic} value of

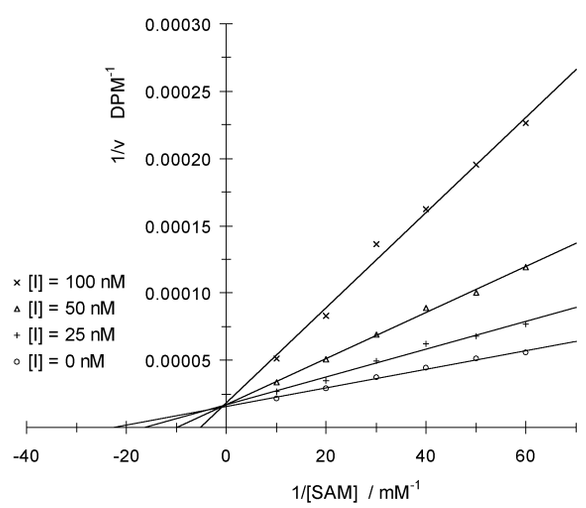

Fig. 2 Lineweaver–Burk plot of reciprocal enzymatic activity *vs.* reciprocal SAM concentration for varying concentrations of inhibitor **2** at saturating benzene-1,2-diol concentration; DPM = decays per minute.

28 ± 2 nM. With respect to the catechol binding site, **2** showed a more complex, mixed inhibition mechanism (Fig. 3). The calculated inhibition constants were K_{ic} = 23 ± 4 nM and K_{iu} = 13 ± 4 μM. The competitive inhibition pattern with respect to the SAM binding site and the mixed inhibition pattern with respect to the catechol site probably indicate an ordered mechanism of inhibition in which occupation of the SAM binding site is first required to allow effective binding to the catechol binding site.[11]

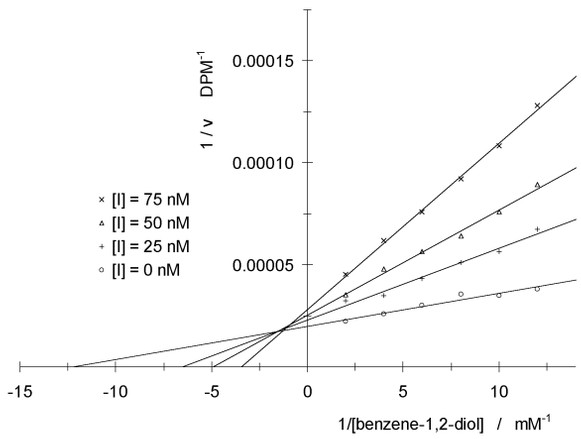

Fig. 3 Lineweaver–Burk plot of reciprocal enzymatic activity *vs.* reciprocal benzene-1,2-diol concentration for varying concentrations of inhibitor **2** at saturating SAM concentration.

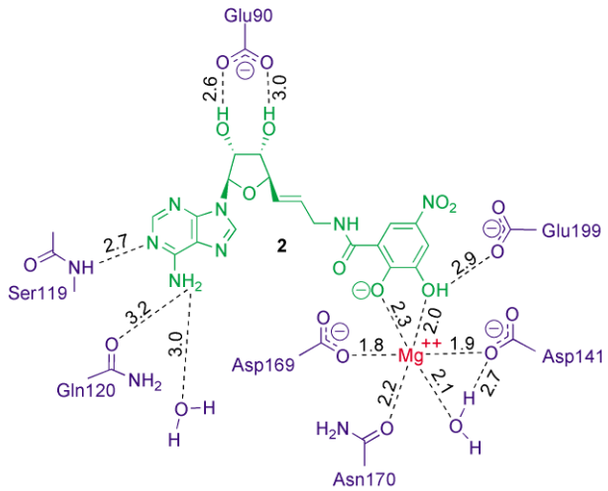

Fig. 5 Schematic drawing of the H-bonding interactions (dashed lines) in the ternary complex. Distances are given in Ångstroms (Å).

Details of the bisubstrate binding mode as revealed by X-ray crystallography

For structural characterisation, COMT was co-crystallised with inhibitor **2** and Mg^{++} ions. The X-ray crystal structure of the ternary complex was refined at 2.6 Å resolution using the program CNX.[13] Bond distances to the Mg ion were not restrained during refinement. A total of 88.9% of all residues are located in the most favoured regions of the Ramachandran plot with Tyr68 being the only residue in a disallowed region. Atomic coordinates are available from the Brookhaven Protein Databank, with the PDB entry code 1JR4. The protein structure in the ternary complex resembles that of the quaternary complex of COMT[10,11] with SAM, 3,5-dinitrocatechol, and a Mg^{2+} ion, with an overall root mean square (r.m.s.) deviation for the Cα atoms of 0.4 Å. The electron density reveals crystallographic disorder about the side chain of Trp143. As shown in Fig. 4, the

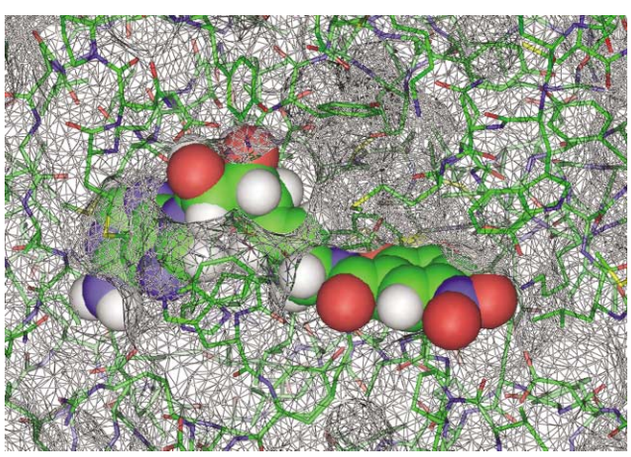

Fig. 4 The active site region in the X-ray crystal structure of the ternary complex between COMT, Mg^{2+} ion and inhibitor **2**. Space filling representation of **2** and solvent-accessible surface of COMT. It is clearly seen how the indole ring of Trp143 shields the adenosine and linker binding from exterior solvent.

bisubstrate inhibitor fills both the nucleoside and the catechol binding pockets. Fig. 5 shows a schematic representation of the hydrogen bonding in the ternary complex.

The adenine moiety has a favourable edge-to-face contact (shortest C ··· C distance: 3.5 Å) with the indole moiety of Trp143 which is located on the surface of COMT and shields the nucleobase and the linker from exterior bulk solvent (Fig. 6). The nucleobase is sandwiched between the imidazole ring of His142, deeply located in the enzyme, and the side chain of Met91 (Fig. 6). Whereas the imidazole ring undergoes a favourable C_{His}–H ··· π interaction with the adenine nucleus (centre-to-centre distance between the two ring systems: 5.1 Å), the methionine side chain stacks atop the six-membered ring of the nucleobase, with a closest intermolecular S ··· C contact of 3.6 Å. Close intermolecular interactions between methionine side chains, with their highly polarisable S-atom, and nucleobases are frequently observed in kinases[28] and other nucleobase-binding enzymes.[29]

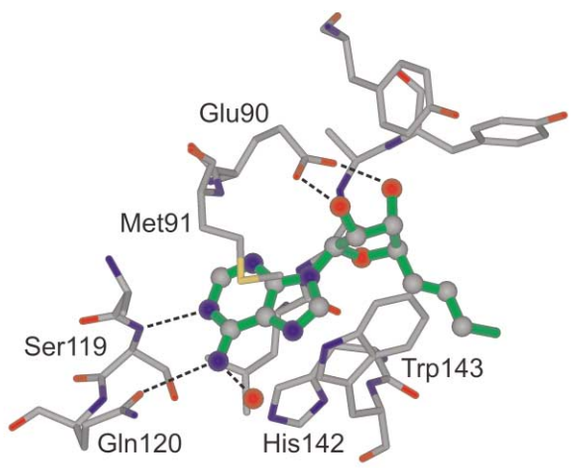

Fig. 6 The nucleoside binding region in the X-ray crystal structure of the ternary complex. Hydrogen bonds are represented as dashed lines.

The NH_2 group of adenine forms hydrogen bonds to the side chain amide C=O of Gln120 and a fixed H_2O molecule, whereas N(1) undergoes hydrogen-bonding to the backbone N–H of Ser119 (for distances see Fig. 5). The two short ionic H-bonds of the 2′,3′-OH groups of the ribose moiety to the carboxylate of Glu90 seem to be quite essential in the recognition of the inhibitor by the enzyme. We found that removal of one of these OH-groups in **2** dramatically decreases the inhibitory affinity.[30]

In the catechol binding pocket (Fig. 7), the Mg^{2+} ion is coordinated octahedrally to the side chains of Asp141, Asp169 and Asn170, one localized H_2O molecule and the two OH groups of the catechol moiety. The OH group in *para* position to the electron withdrawing nitro group is most probably deprotonated (measured pK_a in aqueous solution = 4.4; it can be expected that coordination to the Mg^{2+} ion leads to a further increase in acidity) whereas the other one forms a H-bond to the carboxylate of Glu199. The nitro group has favourable van der Waals contacts to Pro174. The side chain of Met40 shields the catechol and parts of the linker from the exterior, and its methyl group is rotated by 79° relative to the conformation of Met40 found in the quaternary complex of COMT.

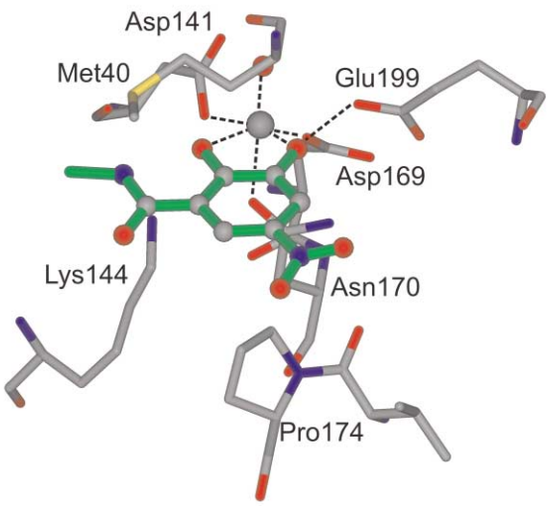

Fig. 7 The catechol binding region in the X-ray crystal structure of the ternary complex. Hydrogen bonds are represented as dashed lines.

Conclusions

Bisubstrate inhibition is a powerful concept to enhance binding affinity and selectivity for therapeutically relevant enzymes that catalyse reactions of two or more substrates or of a substrate and a cofactor. This is clearly demonstrated in the present study, which reports the versatile synthesis of a very potent bisubstrate inhibitor (**2**) for COMT with an IC_{50} value of 9 nM. The bisubstrate binding mode of **2** was proven in kinetic studies and by X-ray crystal structure analysis. This breakthrough could lead to novel effective drugs against the symptoms of Parkinson's disease.

In order to accommodate in a strain-free way both the nucleoside and the catechol moieties at their respective binding sites, the size of the linker between them requires an optimal length. In this particular study, linkers consisting of one (too short; **3**) or four carbon atoms (too long; **6**) only led to inhibitors with micromolar activities, whereas linkers with two (**4**) or three (**5**) carbon atoms are active in the nanomolar range. The olefinic three-carbon spacer in **2** leads to further enhanced binding affinity since the inhibitor is highly preorganised prior to complexation, being unable to undergo hydrophobic collapse in the unbound state. The results of this investigation strongly advise to consider both the unbound and bound state in the optimisation of a new inhibitor. Thus the present findings are of considerable interest for the development of inhibitors for kinases and other methyltransferases that also require, in addition to a substrate, a cofactor for function and are popular targets in modern medicinal chemistry. We are now focusing on structural variations of the ribose, catechol and nucleobase moieties in next-generation bisubstrate inhibitors for COMT and are exploring the extension of the gained knowledge to other enzymes.

Experimental

General details

Solvents and reagents were purchased reagent-grade and used without further purification. All reactions were carried out under an Ar atmosphere. The following compounds were prepared according to literature procedures: *N*-hydroxysuccinimide ester **7**,[11] 5′-amino-2′,3′-*O*-isopropylidene-5′-deoxyadenosine (**8**),[17] 2′,3′-*O*-isopropylideneadenosine (**9**),[18] and *o*-iodoxybenzoic acid (IBX).[31] THF was freshly distilled from sodium benzophenone ketyl, CH_2Cl_2 from CaH_2. Anhydrous Me_2SO and DMF, stored over molecular sieves, were purchased from Fluka. Evaporation *in vacuo* was done at *ca.* 20 Torr. All products were dried under high vacuum (0.05 Torr) before analytical characterisation. Thin layer chromatography was performed on glass plates coated with Merck SiO_2 60 F_{254}. Column chromatography was performed using Fluka SiO_2 60 (230–400 mesh, 0.040–0.063 mm). Reversed-phase column chromatography was done using Fluka silica gel 100 C_{18} (230–400 mesh, 0.040–0.063 mm). Analytical reversed-phase HPLC was performed on a LiChrospher C-18 column (250 × 4 mm, 5 µm, 100 Å) from Merck, eluted with a linear gradient of 5% MeCN in water containing 0.1% TFA to 100% MeCN during 20 min and a flow-rate of 1 cm^3 min^{-1} (UV detection at 254 nm). Melting points were determined with a Büchi B-540 melting point apparatus and are uncorrected. Optical rotations were measured on a Perkin–Elmer 241 polarimeter at λ = 589 nm or λ = 578 nm and are given in 10^{-1} deg cm^2 g^{-1}. Infrared spectra were recorded on a Perkin–Elmer 1600-FT–IR spectrometer. ^1H and ^{13}C NMR spectra (δ [ppm]; J [Hz]) were recorded on Varian Gemini 300 and Varian Mercury 300 spectrometers. MALDI mass spectra were recorded on an IonSpec Ultima instrument using 2,5-dihydroxybenzoic acid or 2,4,5-trihydroxyacetophenone–diammonium citrate (2:1) as a matrix. The nomenclature was generated with the computer program ACD-Name (ACD/Labs).

N-{[(2*R*,3*S*,4*R*,5*R*)-5-(6-Amino-9*H*-purin-9-yl)-3,4-dihydroxytetrahydrofuran-2-yl]methyl}-2,3-dihydroxy-5-nitrobenzene-1-carboxamide (3)

To **8** (89 mg, 0.34 mmol) in dry DMF (5 cm^3), Et_3N (0.1 cm^3, 1 mmol) and **7** (110 mg, 0.372 mmol) were added and the resulting red solution was stirred at 20 °C for 15 h. Water (100 cm^3) was added and the mixture adsorbed on a column with reversed-phase SiO_2 (1 cm × 25 cm). After washing with 1% aq. HCOOH (200 cm^3), **3** was eluted with CH_3CN–1% aq. HCOOH (2:8 ⟶ 3:8). Evaporation to dryness by lyophilisation and re-precipitation of the residue from MeOH–Et_2O afforded **3** (130 mg, 86%) as an orange powder, mp 198 °C (MeOH–Et_2O); HPLC t_R 7.02 min; $[a]_D^{20}$ −27 (*c.* 0.33 in Me_2SO); ν_{max}(KBr)/cm^{-1} 3363s, 3204s, 1647s, 1506s, 1473s, 1333s, 1175m, 1129m, 1072m, 855w, 825w, 769w, 743w, 649w; δ_H(300 MHz; $(CD_3)_2SO$ + 1 drop of CF_3COOD) 3.62–3.75 (2 H, m), 4.15 (1 H, dd, J 10.3, 5.3), 4.24 (1 H, t, J 5.3), 4.67 (1 H, t, J 5.3), 5.97 (1 H, d, J 5.3), 7.72 (1 H, d, J 2.5), 8.38 (1 H, d, J 2.5), 8.43 (1 H, s), 8.73 (1 H, s), 9.31 (1 H, t, J 5.0); δ_C(75 MHz; $(CD_3)_2SO$) 41.7, 71.6, 73.2, 82.9, 88.2, 111.3, 115.1, 115.7, 119.6, 137.7, 140.4, 147.3, 149.6, 152.2, 155.9, 157.3, 168.1; HRMS (MALDI) calcd. for $C_{17}H_{18}N_7O_8^+$ (MH^+): 448.1217; found: 448.1208.

2-{(3a*R*,4*R*,6*R*,6a*R*)-6-(6-Amino-9*H*-purin-9-yl)-2,2-dimethylperhydrofuro[3,4-*d*][1,3]dioxol-4-yl}ethanenitrile (10)

To a well stirred suspension of **9** (758 mg, 2.47 mmol) and PPh_3 (1.617 g, 6.166 mmol) in THF (12.4 cm^3), acetone cyanohydrin (0.57 cm^3, 6.2 mmol) was added. Within 5 min, DEAD (0.98 cm^3, 97%, 6.1 mmol) was added at 0 °C. The solution was stirred at 0 °C for 50 min and further at 20 °C for 16 h. Evaporation *in vacuo* and column chromatography (SiO_2; EtOAc–MeOH (96:4)) afforded **10** (698 mg, 89%) as a brown oil; δ_H(200 MHz; $CDCl_3$) 1.42 (3 H, s), 1.64 (3 H, s), 2.84–3.08 (2 H, m), 4.51–4.60 (1 H, m), 5.16 (1 H, dd, J 6.2, 3.3), 5.50 (1 H, dd, J 6.2, 2.1), 5.71 (2 H, br s), 6.12 (1 H, d, J 2.1); 7.93 (1 H, s); 8.38 (s, 1 H).

(2*R*,3*S*,4*R*,5*R*)-2-(2-Aminoethyl)-5-(6-amino-9*H*-purin-9-yl)-tetrahydrofuran-3,4-diol (11)

To a 0.1 M solution of **10** in THF (11 cm^3, 1.1 mmol), glacial acetic acid (20 cm^3) and PtO_2 (200 mg) were added. The suspension was hydrogenated (4 bar H_2) for 19 h. The catalyst was removed by filtration and the solvent evaporated *in vacuo*.

Water (4 cm^3) and TFA (10 cm^3) were added to the residue, and the resulting solution was stirred for 2 h at 20 °C. The mixture was diluted with water (300 cm^3) and extracted with $CHCl_3$ (3 × 100 cm^3). The aqueous phase was evaporated *in vacuo* to give a residue that was dissolved in water (10 cm^3) and loaded onto a column of Dowex® 50 Wx4 (NH_4^+, 1 cm × 25 cm). Washing with MeOH–H_2O (1:1, 400 cm^3) and elution with MeOH–13% aq. NH_3 (1:1), followed by removal of MeOH *in vacuo*, left an aqueous product-containing solution that was lyophilised to give **11** (227 mg, 74%) as a brown foam; δ_H(300 MHz; CD_3OD + 1 drop of CF_3COOD) 2.14–2.18 (2 H, m), 3.10 (2 H, t, *J* 6.9), 4.10–4.14 (1 H, m), 4.27 (1 H, t, *J* 4.5), 4.67 (1 H, t, *J* 4.5), 6.04 (1 H, d, *J* 4.1), 8.40 (1 H, s), 8.44 (1 H, s).

N-{2-[(2*R*,3*S*,4*R*,5*R*)-5-(6-Amino-9*H*-purin-9-yl)-3,4-dihydroxytetrahydrofuran-2-yl]ethyl}-2,3-dihydroxy-5-nitrobenzene-1-carboxamide (4)

Starting from **11** (100 mg, 0.357 mmol) and **7** (116 mg, 0.392 mmol), the procedure described for **3** afforded **4** (161 mg, 98%) as an orange powder, mp 150 °C (decomp.) (Et_2O–MeOH); HPLC t_R 7.89 min; $[\alpha]_D^{20}$ −11 (*c.* 0.5 in Me_2SO); ν_{max}(KBr)/cm^{-1} 3332s, 1696s, 1560w, 1516m, 1475w, 1420w, 1333s, 1201s, 1135m, 893w, 838w, 800w, 744w, 723m; δ_H(300 MHz; $(CD_3)_2SO$ + 1 drop of CF_3COOD) 1.97–2.10 (2 H, m), 3.36–3.48 (2 H, m), 4.03–4.10 (2 H, m), 4.61 (1 H, t, *J* 4.7), 5.97 (1 H, d, *J* 4.7), 7.69 (1 H, d, *J* 2.5), 8.33 (1 H, d, *J* 2.5), 8.45 (1 H, s), 8.65 (1 H, s); δ_C(75 MHz; $(CD_3)_2SO$) 32.4, 36.3, 73.2, 73.3, 81.9, 87.9, 111.9, 114.1, 114.2, 118.9, 138.2, 141.6, 146.8, 147.6, 148.5, 152.2, 156.1, 168.0; HRMS (MALDI) calcd. for $C_{18}H_{20}N_7O_8^+$ (MH^+): 462.1373; found: 462.1364.

Ethyl (*E*)-3-{(3a*R*,4*R*,6*R*,6a*R*)-6-(6-amino-9*H*-purin-9-yl)-2,2-dimethylperhydrofuro[3,4-*d*][1,3]dioxol-4-yl}prop-2-enoate (12)

To **9** (12.3 g, 40 mmol) in Me_2SO (100 cm^3), $Ph_3P{=}CHCO_2Et$ (42.8 g, 100 mmol) and *o*-iodoxybenzoic acid (IBX) (27.8 g, 100 mmol) were added. The mixture was stirred at 20 °C for 72 h. Water (500 cm^3) was added and the mixture extracted with EtOAc (2 × 500 cm^3). The combined organic phases were dried (Na_2SO_4) and concentrated to a residue which was purified by column chromatography (SiO_2; EtOAc–MeOH (96:4)) to give **12** (10.5 g, 70%) as colorless crystals, mp 102 °C (EtOH) (lit.,[22] 104–106 °C); δ_H(300 MHz; $CDCl_3$) 1.22 (3 H, t, *J* 7.2), 1.40 (3 H, s), 1.63 (3 H, s), 4.11 (2 H, q, *J* 7.2), 4.79–4.83 (1 H, m), 5.14 (1 H, dd, *J* 6.2, 3.4), 5.56 (1 H, dd, *J* 6.2, 1.9), 5.81 (1 H, dd, *J* 15.9, 1.7), 6.13 (1 H, d, *J* 1.9), 6.96 (1 H, dd, *J* 15.9, 5.6), 7.87 (1 H, s), 8.33 (1 H, s).

(*E*)-3-{(3a*R*,4*R*,6*R*,6a*R*)-6-(6-Amino-9*H*-purin-9-yl)-2,2-dimethylperhydrofuro[3,4-*d*][1,3]dioxol-4-yl}prop-2-en-1-ol (13)

To **12** (375 mg, 1 mmol) in CH_2Cl_2 (3 cm^3), a 1 M solution of DIBAL-H in hexane (8 cm^3, 8 mmol) was added dropwise. The mixture was stirred at −78 °C for 2 h and then quenched with MeOH (5 cm^3). A saturated aqueous solution of potassium sodium tartrate monohydrate (Rochelle salt, 50 cm^3) was added, and the resulting suspension was stirred vigorously for 16 h at 20 °C, then extracted with EtOAc (3 × 50 cm^3). The combined organic phases were dried (Na_2SO_4) and evaporated to dryness *in vacuo* to afford **13** (328 mg, 98%) as a colorless foam; $[\alpha]_D^{20}$ 17.8 (*c.* 1 in $CHCl_3$); ν_{max}(KBr)/cm^{-1} 3339s, 2982m, 2932m, 1646s, 1595m, 1472w, 1370w, 1210m, 1080m; δ_H(300 MHz; $CDCl_3$) 1.40 (3 H, s), 1.63 (3 H, s), 4.07 (2 H, s), 4.72 (1 H, dd, *J* 4.1, 2.5), 5.02 (1 H, dd, *J* 6.2, 4.1), 5.54 (1 H, dd, *J* 6.2, 2.2), 5.56 (2 H, s), 5.85–5.87 (2 H, m), 6.10 (1 H, d, *J* 2.2), 7.88 (1 H, s), 8.37 (1 H, s); δ_C(75 MHz; $CDCl_3$) 25.3, 27.0, 61.7, 84.3, 84.6, 87.8, 90.7, 114.3, 119.8, 126.9, 134.4, 139.9, 149.2, 153.1, 155.6; HRMS (MALDI) calcd. for $C_{15}H_{20}N_5O_4^+$ (MH^+): 334.1515; found: 334.1505.

2-(*E*)-3-{(3a*R*,4*R*,6*R*,6a*R*)-6-(6-Amino-9*H*-purin-9-yl)-2,2-dimethylperhydrofuro[3,4-*d*][1,3]dioxol-4-yl}prop-2-enyl-2,3-dihydro-1*H*-isoindole-1,3-dione (14)

DEAD (0.234 cm^3, 97%, 1.46 mmol) was added dropwise to a stirred suspension of **13** (490 mg, 1.46 mmol), phthalimide (215 mg, 1.46 mmol) and Ph_3P (383 mg, 1.46 mmol) in THF (7 cm^3). After stirring for 1.5 h at 20 °C, a colorless solid started to precipitate. Stirring was continued for 1 h, after which the mixture was cooled to 0 °C and filtered. The residue was washed with Et_2O and dried *in vacuo* to give **14** (461 mg, 68%) as colorless crystals, mp 215 °C (MeOH); $[\alpha]_D^{20}$ 9.0 (*c.* 1 in $CHCl_3$); ν_{max}(KBr)/cm^{-1} 3304m, 3155m, 1712s, 1676s, 1603m, 1430m, 1401m, 1335m, 1299m, 1207s, 1079s; δ_H(300 MHz; $CDCl_3$) 1.36 (3 H, s), 1.59 (3 H, s), 4.19 (2 H, d, *J* 5.3), 4.69 (1 H, dd, *J* 6.5, 3.1), 4.98 (1 H, dd, *J* 6.2, 3.1), 5.49 (1 H, dd, *J* 6.2, 2.0), 5.59 (2 H, br s), 5.73 (1 H, dt, *J* 15.6, 5.3), 5.84 (1 H, dd, *J* 15.6, 6.5), 6.07 (1 H, d, *J* 2.0), 7.71–7.76 (2 H, m), 7.80–7.86 (3 H, m), 8.24 (1 H, s); δ_C(75 MHz; $CDCl_3$) 25.3, 27.1, 38.7, 84.2, 84.6, 87.2, 90.6, 114.4, 120.2, 123.4, 127.4, 130.4, 132.0, 134.0, 139.8, 149.4, 153.2, 155.6, 167.7; HRMS (MALDI) calcd. for $C_{23}H_{23}N_6O_5^+$ (MH^+): 463.1730; found: 463.1724.

9-{(3a*R*,4*R*,6*R*,6a*R*)-6-[(*E*)-3-Aminoprop-1-enyl]-2,2-dimethylperhydrofuro[3,4-*d*][1,3]dioxol-4-yl}-9*H*-purin-6-amine (15)

To phthalimide **14** (885 mg, 1.91 mmol), a solution of 33% $MeNH_2$ in EtOH (30 cm^3) was added and the mixture was stirred at 20 °C for 16 h. After evaporation *in vacuo*, the residue was dissolved in $CHCl_3$ (25 cm^3) and extracted with 10% aqueous AcOH (30 cm^3). The aqueous phase was washed with $CHCl_3$ (3 × 25 cm^3), adjusted to pH > 12 with 2 N NaOH and then extracted again with $CHCl_3$ (4 × 25 cm^3). The combined organic phases were dried (Na_2SO_4) and evaporated to give **15** (605 mg, 95%) as a colorless foam; $[\alpha]_D^{20}$ 30.8 (*c.* 1 in $CHCl_3$); ν_{max}(KBr)/cm^{-1} 3686m, 3414m, 2999m, 1715m, 1631s, 1469w, 1376m, 1087s; δ_H(300 MHz; $CDCl_3$) 1.39 (3 H, s), 1.62 (3 H, s), 3.22 (2 H, d, *J* 5.1), 4.68 (1 H, dd, *J* 7.3, 3.4), 4.99 (1 H, dd, *J* 6.2, 3.4), 5.53 (1 H, dd, *J* 6.2, 2.2), 5.71 (1 H, dd, *J* 15.6, 7.3), 5.83 (1 H, dt, *J* 15.6, 5.1), 5.87 (2 H, br s), 6.08 (1 H, d, *J* 2.2), 7.87 (1 H, s), 8.35 (1 H, s); δ_C(75 MHz; $CDCl_3$) 25.4, 27.2, 43.3, 84.2, 84.6, 87.7, 90.4, 114.4, 120.2, 126.0, 136.3, 139.7, 149.3, 153.0, 155.4; HRMS (MALDI) calcd. for $C_{15}H_{21}N_6O_3^+$ (MH^+): 333.1675; found: 333.1667.

(2*R*,3*S*,4*R*,5*R*)-2-[(*E*)-3-Aminoprop-1-enyl]-5-(6-amino-9*H*-purin-9-yl)tetrahydrofuran-3,4-diol (16)

A solution of **15** (481 mg, 1.45 mmol) in TFA–H_2O (5:2, 14 cm^3) was stirred at 20 °C for 1 h and then evaporated to dryness. Purification of the residue by ion-exchange chromatography as described for **11** gave **16** (339 mg, 80%) as a colorless foam; $[\alpha]_D^{20}$ 65.0 (*c.* 1 in MeOH); ν_{max}(KBr)/cm^{-1} 3286br s, 1704s, 1507m, 2429m, 1325w, 1209s, 1142s, 1052m, 975w, 838m, 800m, 724s; δ_H(300 MHz; D_2O + 1 drop of CF_3COOD) 3.55 (2 H, d, *J* 6.2), 4.28 (1 H, dd, *J* 5.9, 5.0), 4.51 (1 H, t, *J* 5.0), 4.68 (1 H, dd, *J* 5.0, 4.1), 5.81–6.01 (2 H, m), 6.05 (1 H, d, *J* 4.1), 8.32 (1 H, m), 8.33 (1 H, s); δ_C(75 MHz; D_2O) 44.2, 76.2, 76.3, 87.0, 90.4, 121.4, 129.6, 137.5, 142.4, 151.3, 155.4, 158.1; HRMS (MALDI) calcd. for $C_{12}H_{17}N_6O_3^+$ (MH^+): 293.1362; found: 293.1357.

N-{(*E*)-3-[(2*R*,3*S*,4*R*,5*R*)-5-(6-Amino-9*H*-purin-9-yl)-3,4-dihydroxytetrahydrofuran-2-yl]prop-2-enyl}-2,3-dihydroxy-5-nitrobenzene-1-carboxamide (2)

Starting from **16** (29 mg, 0.1 mmol) and **7** (30 mg, 0.1 mmol), the procedure described for **3** afforded **2** (39 mg, 82%) as an orange powder, mp 173 °C (2-propanol); HPLC t_R 9.31 min; $[\alpha]_D^{20}$ −9 (*c.* 0.5 in Me_2SO); ν_{max}(KBr)/cm^{-1} 3378br s, 3115m,

1700s, 1642s, 1514m, 1473s, 1427m, 1351s, 1203s, 1131s, 1049m, 972w; δ_H(300 MHz; $(CD_3)_2SO$) 3.92–4.03 (2 H, m), 4.08–4.16 (1 H, m), 4.35 (1 H, t, *J* 5.3), 4.64–4.74 (1 H, m), 5.23 (1 H, br s), 5.52 (1 H, br s), 5.79–5.96 (3 H, m), 7.34 (2 H, br s), 7.65 (1 H, d, *J* 2.5), 8.07 (1 H, s), 8.32 (1 H, s), 8.48 (1 H, d, *J* 2.5), 9.64 (1 H, br s); δ_C(125 MHz; $(CD_3)_2SO$) 40.3, 72.8, 74.0, 84.0, 87.6, 111.0, 114.2, 115.3, 119.2, 129.0, 129.6, 137.2, 140.0, 147.2, 149.3, 152.3, 155.9, 157.7, 167.7; HRMS (ESI) calcd. for $C_{19}H_{20}N_7O_8^+$ (MH^+): 474.1373; found: 474.1358.

(2*R*,3*S*,4*R*,5*R*)-2-(3-Aminopropyl)-5-(6-amino-9*H*-purin-9-yl)-tetrahydrofuran-3,4-diol (17)

The allylic amine **15** (125 mg, 0.376 mmol) in EtOH (10 cm^3) was hydrogenated (4 bar H_2) in the presence of 10% Pd/C (100 mg) for 18 h. The catalyst was removed by filtration and the solvent evaporated *in vacuo*. TFA–H_2O (5:2, 30 cm^3) was added and the mixture stirred for 1 h at 20 °C, then evaporated to dryness. Purification by ion-exchange chromatography as described for **11** gave **17** (94 mg, 84%) as a yellow foam; $[a]_D^{20}$ −11.3 (*c.* 1 in MeOH); ν_{max}(KBr)/cm^{-1} 3105br s, 1695s, 1506m, 1431s, 1322m, 1206s, 1128s, 1061m, 839m, 800m, 717m; δ_H(300 MHz; CD_3OD) 1.75–1.87 (4 H, m), 2.97 (2 H, t, *J* 7.5), 4.00–4.05 (1 H, m), 4.21 (1 H, t, *J* 5.0), 4.78 (1 H, t, *J* 5.0), 5.97 (1 H, d, *J* 5.0), 8.19 (1 H, s), 8.24 (1 H, s); δ_C(75 MHz; CD_3OD) 25.2, 31.1, 40.4, 74.6, 74.8, 84.9, 90.2, 120.5, 141.4, 150.4, 153.7, 157.1; HRMS (MALDI) calcd. for $C_{12}H_{19}N_6O_3^+$ (MH^+): 295.1519; found: 295.1508.

***N*-{3-[(2*R*,3*S*,4*R*,5*R*)-5-(6-Amino-9*H*-purin-9-yl)-3,4-dihydroxytetrahydrofuran-2-yl]propyl}-2,3-dihydroxy-5-nitrobenzene-1-carboxamide (5)**

Starting from **17** (10 mg, 0.038 mmol) and **7** (11 mg, 0.038 mmol), the procedure described for **3** afforded **5** (16 mg, 89%) as a yellow foam; HPLC t_R 9.20 min; $[a]_D^{20}$ −55 (*c.* 1.0 in THF); ν_{max}(KBr)/cm^{-1} 3340br s, 1706s, 1646s, 1475s, 1263s, 1077m, 796w; δ_H($(CD_3)_2SO$ + 1 drop of CF_3COOD) 1.60–1.73 (4 H, m), 3.30–3.40 (2 H, m), 3.91–3.95 (1 H, m), 4.04 (1 H, t, *J* 5.0), 4.58 (1 H, t, *J* 5.0), 5.94 (1 H, d, *J* 5.0), 7.71 (1 H, d, *J* 2.5), 8.42 (1 H, d, *J* 2.5), 8.49 (1 H, s), 8.69 (1 H, s), 9.21 (1 H, br s); δ_C(75 MHz; $(CD_3)_2SO$ + 1 drop of CF_3COOD) 25.0, 30.3, 73.0, 73.4, 83.9, 87.8, 111.8, 113.9, 114.0, 118.6, 138.2, 142.4, 144.5, 146.5, 148.0, 149.7, 155.8, 167.8, one peak missing due to signal overlap; HRMS (MALDI) calcd. for $C_{19}H_{21}N_7O_8^+$ ($[M + Na]^+$): 498.1349; found: 498.1345.

4-{(3a*R*,4*R*,6*R*,6a*R*)-6-(6-Amino-9*H*-purin-9-yl)-2,2-dimethylperhydrofuro[3,4-*d*][1,3]dioxol-4-yl}butanenitrile (18)

The allylic alcohol **13** (267 mg, 0.8 mmol) in EtOH (20 cm^3) was hydrogenated (6 bar H_2) in the presence of 10% Pd/C (100 mg) for 3 h. The catalyst was removed by filtration and the solvent evaporated *in vacuo*. The residue was dissolved in THF (5 cm^3), then PPh_3 (0.51 g, 2.0 mmol) and acetone cyanohydrin (0.18 cm^3, 2.0 mmol) were added. Within 5 min, DEAD (0.3 cm^3, 97%, 1.9 mmol) was added at 0 °C. The solution was stirred at 20 °C for 70 h. The orange mixture was evaporated *in vacuo* to give an oil that was purified by column chromatography (SiO_2; $CHCl_3$–MeOH (96:4)) to provide **18** (131 mg, 49%) as a colorless oil; $[a]_D^{20}$ −2.5 (*c.* 1 in $CHCl_3$); ν_{max}($CHCl_3$)/cm^{-1} 3412m, 1716m, 1632s, 1588m, 1473m, 1376m, 1156m, 1094s; δ_H(300 MHz; $CDCl_3$) 1.34 (3 H, s), 1.56 (3 H, s), 1.63–1.88 (4 H, m), 2.24–2.30 (2 H, m), 4.07–4.14 (1 H, m), 4.85 (1 H, dd, *J* 6.5, 4.0), 5.44 (1 H, dd, *J* 6.5, 2.3), 5.99 (1 H, d, *J* 2.3), 6.49 (2 H, br s), 7.84 (1 H, s), 8.28 (1 H, s); δ_C(75 MHz; $CDCl_3$) 17.0, 21.9, 25.4, 27.2, 32.1, 83.8, 84.0, 85.9, 90.0, 114.6, 119.1, 120.1, 139.6, 149.0, 153.0, 155.8; HRMS (MALDI) calcd. for $C_{16}H_{21}N_6O_3^+$ (MH^+): 345.1675; found: 345.1673.

***N*-{4-[(2*R*,3*S*,4*R*,5*R*)-5-(6-Amino-9*H*-purin-9-yl)-3,4-dihydroxytetrahydrofuran-2-yl]butyl}-2,3-dihydroxy-5-nitrobenzene-1-carboxamide (6)**

Nitrile **18** (122 mg, 0.8 mmol) was hydrogenated and deprotected as described for **4** but the resulting amine was used without purification in the next step. Reaction with **7** (243 mg, 0.82 mmol) as described for **3** afforded **6** (69 mg, 18%) as an orange foam; HPLC t_R 9.72 min; $[a]_{Hg578}^{20}$ +1.0 (*c.* 0.8 in MeOH); ν_{max}(KBr)/cm^{-1} 3384br s, 2941m, 1700 s, 1507m, 1473m, 1340s, 1202s, 1136m, 799w 723m; δ_H(300 MHz; CD_3OD) 1.53–1.87 (6 H, m), 3.41 (2 H, t, *J* 6.2), 4.01–4.07 (1 H, m), 4.14 (1 H, t, *J* 5.0), 4.69 (1 H, t, *J* 5.0), 5.99 (1 H, d, *J* 5.0), 7.72 (1 H, d, *J* 2.5), 8.27 (1 H, d, *J* 2.5), 8.33 (1 H, s), 8.38 (1 H, s); δ_C(75 MHz; CD_3OD) 24.2, 30.0, 34.1, 40.5, 75.1, 75.4, 86.0, 90.5, 113.3, 115.5, 116.1, 120.7, 140.7, 143.6, 147.3, 148.2, 150.2, 153.2, 156.5, 169.8; HRMS (MALDI) calcd. for $C_{20}H_{24}N_7O_8^+$ (MH^+): 490.1686; found: 490.1680.

Enzymatic studies

Full experimental details of the radiochemical assay to determine IC_{50} values and the kinetic measurements for determining the enzyme inhibition mechanisms are given in previous publications.[11,13,27] The procedure for co-crystallizing COMT with inhibitor **2** and Mg^{++} ions and solving the X-ray crystal structure has also been reported.[13]

Acknowledgements

We thank F. Hoffmann-La Roche, Basel for generous support of this work. We are grateful to P. Malherbe for the cloning of COMT, P. Caspers for the expression of COMT, A. Cesura for enzyme purification, B. Wipf for fermentation and H. W. Lahm for sequencing.

References

1 D. Broom, *J. Med. Chem.*, 1989, **32**, 2–7.
2 (*a*) W. T. Miller, *Nat. Struct. Biol.*, 2001, **8**, 16–18; (*b*) K. Parang, J. H. Till, A. J. Ablooglu, R. A. Kohanski, S. R. Hubbard and P. A. Cole, *Nat. Struct. Biol.*, 2001, **8**, 37–41.
3 K. Hinterding, P. Hagenbuch, J. Retey and H. Waldmann, *Chem. Eur. J.*, 1999, **5**, 227–236.
4 M. Schlitzer, M. Bohm and I. Sattler, *Bioorg. Med. Chem.*, 2002, **10**, 615–620.
5 E. Wolf, J. De Angelis, E. M. Khalil, P. A. Cole and S. K. Burley, *J. Mol. Biol.*, 2002, **317**, 215–224.
6 K. L. Levert and G. L. Waldrop, *Biochem. Biophys. Res. Commun.*, 2002, **291**, 1213–1217.
7 (*a*) P. T. Männistö, I. Ulmanen, K. Lundström, J. Taskinen, J. Tenhunen, C. Tilgmann and S. Kaakkola, *Prog. Drug Res.*, 1992, **39**, 291–350; (*b*) P. T. Männistö and S. Kaakkola, *Pharmacol. Rev.*, 1999, **51**, 593–628; (*c*) V. V. Myllylä, M. Jackson, J. P. Larsen and H. Baas, *Eur. J. Neurol.*, 1997, **4**, 333–341; (*d*) M. C. Kurth, C. H. Adler, M. St. Hilaire, C. Singer, C. Waters, P. LeWitt, D. A. Chernik, E. E. Dorflinger and K. Yoo, *Neurology*, 1997, **48**, 81–87; (*e*) H. Baas, A. G. Beiske, J. Ghika, M. Jackson, W. H. Oertel, W. Poewe and G. Ransmayr, *J. Neurol. Neurosurg. Psychiatry*, 1997, **63**, 421–428.
8 J. Borgulya, M. Da Prada, J. Dingemanse, R. Scherschlicht, B. Schläppi and G. Zürcher, *Drugs of the Future*, 1991, **16**, 719–721.
9 E. Nissinen, I. B. Linden, E. Schultz and P. Pohto, *Naunyn-Schmiedebergs Arch. Pharmacol.*, 1992, **346**, 262–266.
10 J. Vidgren, L. A. Svensson and A. Liljas, *Nature*, 1994, **368**, 354–358.
11 B. Masjost, P. Ballmer, E. Borroni, G. Zürcher, F. K. Winkler, R. Jakob-Roetne and F. Diederich, *Chem. Eur. J.*, 2000, **6**, 971–982.
12 For earlier approaches to the development of bisubstrate inhibitors of COMT, see: E. K. Yau and J. K. Coward, *J. Org. Chem.*, 1990, **55**, 3147–3158.
13 For a preliminary communication of parts of this work, see: C. Lerner, A. Ruf, V. Gramlich, B. Masjost, G. Zürcher, R. Jakob-Roetne, E. Borroni and F. Diederich, *Angew. Chem., Int. Ed. Engl.*, 2001, **40**, 4040–4042.
14 B. Masjost, doctoral dissertation ETH No. 13719, Zürich, 2000.
15 D. J. Cram, *Angew. Chem., Int. Ed. Engl.*, 1988, **27**, 1009–1020.

16 P. R. Gerber and K. Muller, *J. Comput.-Aided Mol. Des.*, 1995, **9**, 251–268.
17 M. Kolb, C. Danzin, J. Barth and N. Claverie, *J. Med. Chem.*, 1982, **25**, 550–556.
18 J. Tomasz, in *Nucleic Acid Chemistry*, ed. R. S. Tipson and L. B. Townsend, John Wiley & Sons, New York, 1978, vol. 2, 765–769.
19 J. Hollmann and E. Schlimme, *Liebigs Ann. Chem.*, 1984, 98–107.
20 B. K. Wilk, *Synth. Commun.*, 1993, **23**, 2481–2484.
21 E. J. Delaney, P. W. Morris, T. Matsushita and D. L. Venton, *J. Carbohydr., Nucleosides, Nucleotides*, 1981, **8**, 445–459.
22 A. Matsuda and T. Ueda, *Chem. Pharm. Bull.*, 1986, **34**, 1573–1578.
23 J. A. Montgomery, A. G. Laseter and K. Hewson, *J. Heterocycl. Chem.*, 1974, **11**, 211–214.
24 K. E. Pfitzner and J. G. Moffatt, *J. Am. Chem. Soc.*, 1965, **87**, 5661–5670.
25 D. Crich and X. S. Mo, *Synlett*, 1999, 67–68.
26 S. Wolfe and S. K. Hasan, *Can. J. Chem.*, 1970, **48**, 3572–3579.
27 G. Zürcher and M. Da Prada, *J. Neurochem.*, 1982, **38**, 191–195.
28 (*a*) J. Vogt, R. Perozzo, A. Pautsch, A. Prota, P. Schelling, P. Pilger, G. Folkers, L. Scapozza and G. E. Schulz, *Proteins*, 2000, **41**, 545–553; (*b*) S. Pakhomova, M. Kobayashi, J. Buck and M. E. Newcomer, *Nat. Struct. Biol.*, 2001, **8**, 447–451.
29 (*a*) V. Villeret, S. H. Huang, Y. P. Zhang and W. N. Lipscomb, *Biochemistry*, 1995, **34**, 4307–4315; (*b*) C. Zubieta, X. Z. He, R. A. Dixon and J. P. Noel, *Nat. Struct. Biol.*, 2001, **8**, 271–279; (*c*) A. Ruf, V. Rolli, G. de Murcia and G. E. Schulz, *J. Mol. Biol.*, 1998, **278**, 57–65; (*d*) E. A. Meyer, R. Brenk, R. K. Castellano, M. Furler, G. Klebe and F. Diederich, *ChemBioChem*, 2002, **3**, 250–253.
30 C. Lerner, R. Siegrist and F. Diederich, unpublished results.
31 R. E. Ireland and L. B. Liu, *J. Org. Chem.*, 1993, **58**, 2899–2899.